Evolution of the diffraction pattern during the transition from the near-field toward the far-field region

M. GRABKA[1], S. PUSTELNY[1*], B. WAJNCHOLD[1], W. GAWLIK[1], and P. MERGO[2]

[1] Center for Magneto-Optical Research, Institute of Physics, Jagiellonian University, 4 Reymonta St., 30-059 Kraków, Poland
[2] Deptartment of Optical Fibres Technology, Faculty of Chemistry, Marie Curie-Sklodowska University,
3 Sklodowska Sq., 20-031 Lublin, Poland

Abstract. In the paper we experimentally and theoretically analyze diffraction of light propagating through a microstructured optical fiber on the fiber end face. In the measurements the diffracting light is spatially inhomogeneous and the diffracting object is a solid-state core with a triangular shape. Application of optical system enables detailed experimental investigations of evolution diffraction pattern in the near-field region, in particular, rotation of the observed structure while departing from the fiber end. The experimental results are confirmed with theoretical simulations based on the theory of the Fresnel diffraction.

Key words: wave optics, diffraction of light, near-field diffraction, microstructured optical fibers, photonic-crystal fibers.

1. Introduction

Unique properties of microstructured optical fibers (MOFs), often called photonic-crystal fibers, make them one of the most intensively studied objects of modern optics [1]. The interest is driven by a possibility of tailoring such optical properties of the fibers as dispersion [2], modality [3], mode area [4], nonlinearity (see [5] and reference therein), etc. Modification of MOF's structure allows to control magnitude and sign of the dispersion [6] and fabricate MOFs with zero or negative dispersion in the visible range [7]. Such fibers may, for example, be applied in tunable femtosecond-pulse sources for efficient generation of supercontinuum [8]. The supercontinuum sources have been used in optical coherence tomography [9], metrology [10] and spectroscopy. Another unique property of MOFs is the possibility of filling empty fiber channels with liquids or gases [12]. It may have important practical applications in construction of ultra-low-volume chemical or biological sensors (see, for example [11, 12] and references therein). A particular advantage of the sensors is their increased sensitivity due to long interaction length and enhanced nonlinear interaction thanks to the strong confinement of light. With a strong coupling between light and gas, long interaction length, and high quality of the light beam such nonlinear effects as stimulated Raman scattering [13], electromagnetically induced transparency [14], slow light-pulse propagation [15] may be observed already with ultra-low light powers.

Many of the abovementioned applications require a detailed knowledge of spatial distribution of light transmitted through MOFs. Since the amount of power present in the fiber channels strongly depends on a propagation constant of a mode, this knowledge is essential for determination of the light-matter coupling efficiency. It is particularly important for

solid-core MOFs in which light is guided based on (modified) total internal reflection. In the case light interacts with the channel-filling medium as evanescent wave. The amount of power present in the channels strongly depends on the electromagnetic mode of light and may range from a few percents for fundamental mode up to a dozen or so percents for higher order modes[1]. Reconstruction of the spatial profile of light propagating through the fiber is thus important providing valid information about coupling between light and a filling medium.

A number of techniques were applied for determination of spatial distribution of light in MOFs. In some of these technique the information about the fiber is extracted from measurements of the far-field diffraction pattern [16–18]. In the cases the MOF structures are reduced to step-index fiber with the circular or slab geometry and the refractive index of the cladding equals to the effective refractive index of the fiber. After such reduction, the methods known for analyzing modality of traditional fibers may be applied [19–21]. The other approach bases on analysis of a near-field pattern [22]. Such analysis, however, may be particularly challenging in a case of the fibers with high refractive index contrast where a near-field region extends not further than a few micrometer from the fiber end. Thus in order to obtain detailed information about the near-field distribution the near-field scanning microscopy need to be used [22].

In this paper we theoretically and experimentally analyze diffraction of light on the end face of suspended-core fiber [23]. Such fiber consists of a glass rod of a diameter comparable to the wavelength of light suspended on three thin ($\sim$100 nm thickness) but long ($\geq$10 μm) webs attached to the solid-state cladding. In such a case light is strongly confined in the core and just fractionally penetrates the air channels as

---

evanescent field. Despite the relatively low air-channels filling factor [24], the fibers are very promising for chemical and biological sensing due to their guidance of spectrally broad light (index guiding) and easiness in filling the air channels (see [11] and references therein).

The paper is organized as follows. Section 2 describes the experimental apparatus and the measurement methodology. Section 3 presents results of our experimental and theoretical investigations, as well as a detailed discussion of the similarities and differences between experimentally measured diffraction patterns and patterns calculated based on the theory of Fresnel diffraction. Final remarks are collected in Sec. 4.

2. Experimental setup

The fiber used in our measurements was fabricated in the Laboratory of Optical Fiber Technology at the Marie Curie-Sklodowska University in Lublin [25]. It consists of a triangularly shaped core (1.3-μm diameter of the inscribed circle) supported with 10-μm struts of 100–150-nm width. The core is surrounded by three large (with respect to other characteristics of the fiber) air channels (Fig. 1) that, in principle, may be filled with gas or liquid.
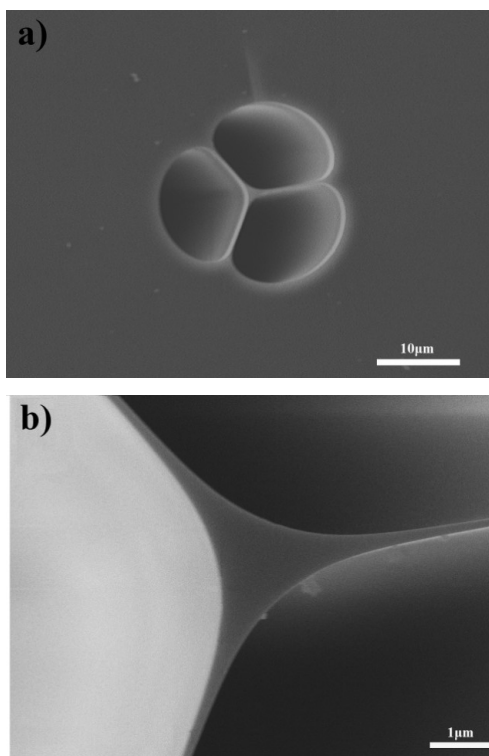

Fig. 1. The scanning electron microscope images of the suspended-core optical fiber used in the measurements. The whole structure of the core is shown in a) while b) is a magnification of the fiber core

Accordingly to the diffraction theory, the nearfield diffraction is observed when $a^2/L\lambda \ll 1$, where a is the diffracting-object characteristic size, L is the distance in which the pattern is observed, and λ is the wavelength of light. In our experimental conditions ($a = 1.3$ μm and $\lambda = 795$ μm), the far-field diffraction is observed for $L \gg 2$ μm or inversely the near-field region ends about 2 μm from the fiber end facet. Since standard CCD camera have photodetectors protected with a glass window and/or filter, it is not usually possible to place it close enough to observe the fiber near-field diffraction pattern (not to mention spatial resolution of the camera required for such measurements). Thus, in order to observe the fiber near-field profile, one needs to construct an optical system [26]. Such a system is used in our experiment (Fig. 2). It consists of the fiber to be visualized, 60x objective (with a numerical aperture of 0.85[2]) mounted at the ultra-precise transitional stage, and the CCD camera. The optical power distribution at the fiber end is reconstituted in a focal plane of the objective (neglecting inhomogeneous waves, which are almost completely attenuated after a few micrometers from the fiber end). Longitudinal motion of the objective displaces the focus in space; In a given plane, e.g. at the position of the beam profiler, different diffraction patterns are observed when objective is shifted. In particular, the images recorded by the profiler enables observation of transition between the near- and far-field regions.
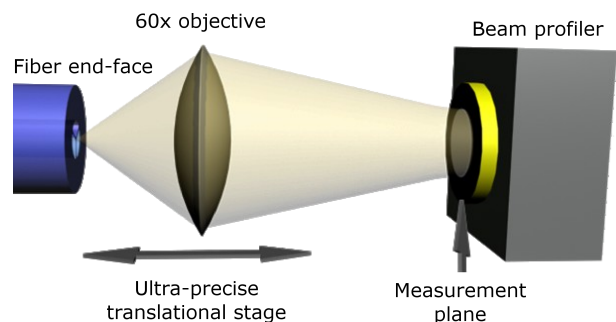

Fig. 2. Simplified diagram of the experimental setup used for fiber-end diffraction pattern measurements. The light is diffracted from the fiber end and it illuminates the 60x objective (NA = 0.85). Longitudinal transition of the objective results in displacement of the focal point of the beam and hence observation of different diffraction pattern on the beam-profiler head

An important advantage of our setup and the applied optical system is expansion of the near-field region and magnification of the observed diffraction pattern in focus of the objective. It facilitates observation of the near-field pattern and transition between diffraction regions. In our experiments the near-field diffraction region is expanded to ~50 μm from the fiber facet and the focal spot is 100 times larger than actual fiber core. The latter property allows to observe the near-field diffraction without further magnification.

3. Results and discussion

We have already stated that the optical system enables observation of the near-field pattern of the fiber and hence recon-

---

[2]Despite of the high numerical aperture of the objective it still is smaller than the numerical aperture of analyzed fiber, 0.8640(79) [26]. Smaller aperture of the objective modifies the fiber diffraction pattern and slightly complicates the problem (see discussion in Sec. 3).

struction of a diffracting object, as well as diffracting-light profile. In our case light of complicated spatial profile is diffracted on the semi-triangular core of the fiber. Since the light is a linear combination of the fiber transverse modes with amplitudes depending on the coupling conditions, length and imperfections of the fiber, a proper description of the diffraction requires knowledge of the transverse mode excited in the fiber. Figure 3 presents the simulations of such first six modes that most significantly contribute to the observed power profiles of the light [27].
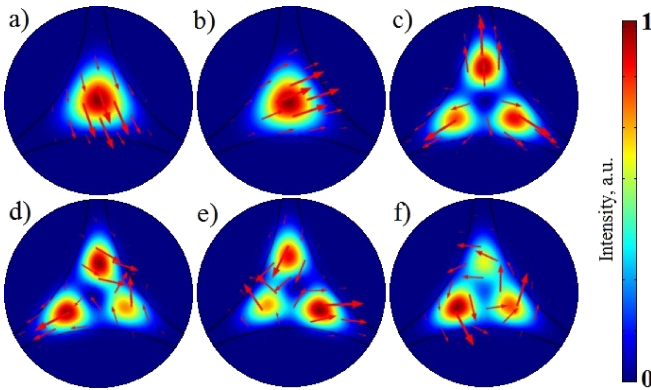

Fig. 3. Simulations of six first transverse modes of the suspended-core fiber that most significantly contribute to the observed spatial power distributions. Arrows represent directions of the electric field

It was shown in [27] that the most efficient coupling of the light into the fiber is obtained when the light beam is focused exactly on the center of the fiber core. It allows one to couple more than 90% of the light (characterize with the Gaussian profile) into the first two (fundamental) modes. For such couplings, the recorded image have almost Gaussian shape with some small, triangular deviations [compare to Fig. 5a].

Diffraction pattern of a given fiber mode can be observed only when a single mode is excited in the fiber, which is a very rare situation; typically many modes are generated in the fiber. Nonetheless, the knowledge of the diffraction profiles of the specific modes provides a good insight into the problem.

Simulated diffraction patterns of four selected modes of our fiber (see Fig. 2) are shown in Fig. 4. These profiles are calculated using a well-known Fresnel diffraction [28]

$$u(x, y, z) = \frac{1}{i\lambda z} e^{ikz} e^{\frac{ik}{2z}(x^2+y^2)}.$$
$$\cdot \int\!\!\!\int\limits_{-\infty}^{+\infty} u(x', y', 0) e^{\frac{ik}{2z}(x'^2+y'^2)} e^{-\frac{ik}{z}(xx'+yy')} dx'dy', \quad (1)$$

where λ is wavelength of the light, $k = 2\pi/\lambda$ the wavenumber of the light, and z the propagation distance. Function u represents the input optical field, where points (x', y') refer to the position at the fiber end, and points (x, y) refer to the position in the image plane. Equation (1) may also be used to

describe Fraunhofer diffraction. In that case the second term under the integral (dependent only on the (x', y') coordinates) is omitted yielding [28]

$$u(x, y, z) = \frac{1}{i\lambda z} e^{ikz} e^{\frac{ik}{2z}(x^2+y^2)}.$$
$$\cdot \int\!\!\!\int\limits_{-\infty}^{+\infty} u(x', y', 0) e^{-\frac{ik}{z}(xx'+yy')} dx'dy'. \quad (2)$$

It is noteworthy that the integral in Eq. (2) is proportional to the two-dimensional Fourier transform of the diffraction optical field.

In general, the transition from the near- toward the far-field region is associated with modification of the observed diffraction patterns. For example, for the fundamental mode (top row in Fig. 4) the near-field profile of the mode is initially described by triangularly-shaped pseudo-Gaussian distribution. This pattern is changing while departing from the fiber end. First the pattern becomes almost perfectly circular, and then recovers its triangular shape being, however, rotated by 180°. The other modes (modes 3, 7, and 13) show similar behavior, i.e. the pattern is rotated by 180°, but the power distributions of light are significantly more complicated.
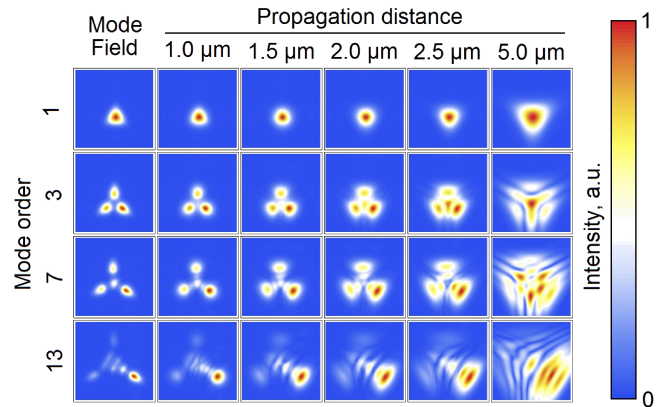

Fig. 4. Simulated near- and far-field diffraction patterns of different modes excited in the suspended-core fiber. Near-field patterns were calculated using Fresnel diffraction theorem while the far-field patterns using the Fraunhofer theorem, i.e. far-field approximation of diffraction equation

Measured profiles follow the same dependence as shown in Fig. 4. For the beam profiler placed in the focal plane of the objective, i.e. in the plane where the fiber facet is reconstructed, the triangularly shaped pseudo-Gaussian pattern is recorded when light is centrally coupled into the fiber and mostly the fundamental modes are excited (Fig. 5). In this case the two vertexes of the recorded triangle lay at a horizontal line and the third vertex is situated above them. While the measurement plane starts to deviate from the focal plane of the objective, the structure first becomes circular and then reappears rotated.

It should be noted that despite many similarities between the measurements and simulations, there are two significant differences. First is the appearance of circular halo in the

M. Grabka, S. Pustelny, B. Wajnchold, W. Gawlik, and P. Mergo

recorded profiles. The rings are a manifestation of the diffraction of light on the circular aperture of the objective, which is associated with slightly smaller numerical aperture of the objective than that of the fiber. Application of the objective with higher numerical aperture should solve the problem. The other difference is in distance at which the transition is observed (almost 10-fold increase of the scale), which results from application of the objective and is highly desirable for enhancing resolution of the measurements.

Figure 6 presents experimentally measured diffraction patterns obtained with light of the spatial profile similar to that of mode 7 (see Fig. 4). Despite the complexity of the measured and simulated patterns some similarities between them may be shown, e.g., similar inhomogeneous distribution of light within the pattern and rotation of the structure while departing from the focal plane/fiber end. The deviations between the dependences originate from the fact that real profile of light contains more contribution than that of 7th mode only.

Based on Eq. (1) it can be easily shown that calculation of

diffraction patterns of light of arbitrary spatial profile on any object is possible. Therefore it is, in general, possible to calculate diffraction of light propagating through the fiber on its end face. However, in order to do so, one needs to find a real power profile of the diffracting light at the fiber end, i.e., evaluate complex amplitudes[3] characterizing contributions of all modes forming the resultant mode. As shown in [27], determination of the light coupled into a specific mode is possible based on the knowledge of the spatial distribution of coupling light its incidence angle, polarization and relative position to the fiber core center.

Although evaluating the energy distribution among the modes is challenging, it can be performed with careful adjustment of the parameter. Exemplary diffraction patterns obtained for the light focused $\sim 1\ \mu$m from the fiber center is shown in Fig. 7. In such a case as many as 5 modes are excited and propagate along the fiber. Simulations of diffraction of such spatially profiled light is shown in Fig. 8. Both simulations and measurements show striking resemblances.
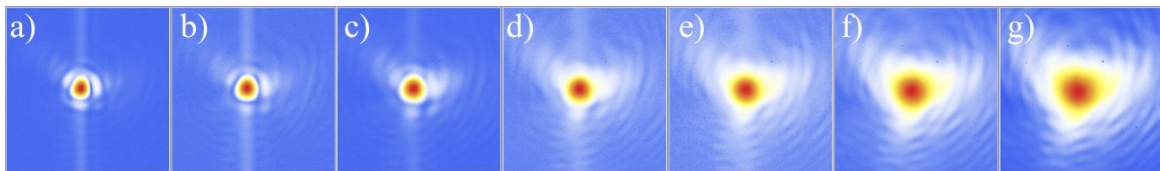

Fig. 5. Measured diffraction profiles a)–g) at different positions of the objective: a) 0.0 μm, b) 7.5 μm, c) 15.0 μm, d) 22.5 μm, e) 30.0 μm, f) 37.5 μm, g) 45.0 μm. Position 0.0 μm corresponds to a measurement in the focal plane. Color scale same as in Fig. 4
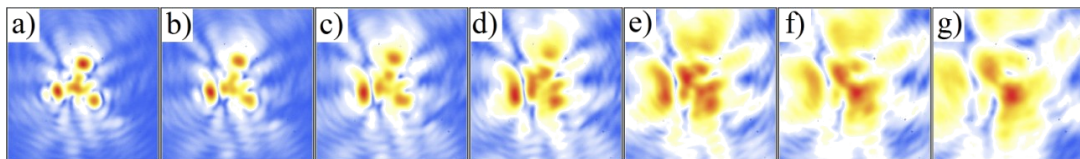

Fig. 6. Measured images obtained for non-optimal coupling conditions, when higher order modes are also excited. Images a)–g) are recorded for different position relative to the focus: a) 0.0 μm, b) 3.0 μm, c) 6.0 μm, d) 10.0 μm, e) 15.0 μm, f) 20.0 μm, g) 30.0 μm. Color scale the same as above
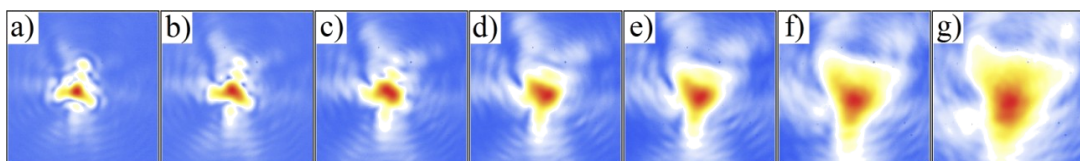

Fig. 7. Measured images obtained for not optimal coupling conditions. Images a)–g) are recorded for different position relative to the focus: a) 0.0 μm, b) 4.0 μm, c) 8.0 μm, d) 13.0 μm, e) 18.0 μm, f) 26.0 μm, g) 36.0 μm
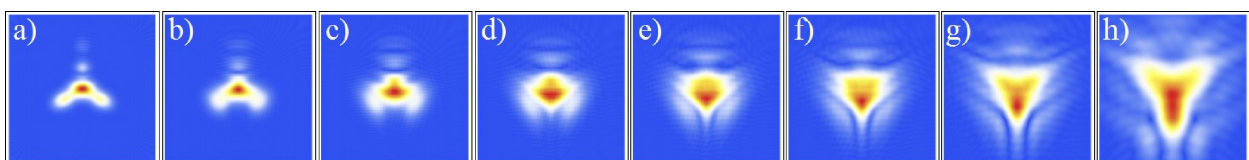

Fig. 8. Simulations results refferring to the measurements from Fig. 7. Different images taken for different distance from the focus: a) 0.0 μm, b) 1.0 μm, c) 1.5 μm, d) 2.0 μm, e) 2.5 μm, f) 3.0 μm, g) 4.0 μm, h) 6.0 μm

---

[3]The amplitudes hold information about the efficiency of coupling light into a given mode, as well as its attenuation and dispersion.

4. Conclusions

We have experimentally and theoretically studied the near-field diffraction of light onto the end face of the suspended-core optical fiber. It was shown that depending on the coupling conditions different transverse modes that are excited in the fibers, which leads to strong modification of the observed diffraction patterns. We also demonstrated that axial departure from the fiber end, which was realized by shifting the position of the objective in our optical system, resulted in the modification of the observed diffraction pattern. In particular, the pattern was reshaped and eventually rotated by 180° when the distance between the objective and beam profiler (effectively fiber end and CCD camera) was significantly increased. All these experimental observations were supported with theoretical calculations

The technique seems to be promising in reconstruction of spatial distribution of light propagating through the fiber. Based on iterative algorithms may evaluate complex coefficient characterizing contribution of a specific mode into the resultant light profile in the fiber, and hence estimate losses and intra-coupling of specific modes. Information about the phase difference between the modes may not only provide important information about the fiber but also might open possibility of independent phase modulation of fiber transverse modes.

REFERENCES

[1] P. Russell, "Photonic crystal fibers", *Science* 299, 358–362 (2003).

[2] T.M. Monro, D.J. Richardson, N.G.R. Broderick, and P.J. Bennett, "Holey optical fibers: an efficient modal model", *J. Lightwave Technol.* 17, 1093–1101 (1999).

[3] T.A. Birks, J.C. Knight, and P.S. Russell, "Endlessly single-mode photonic crystal fiber", *Opt. Lett.* 22, 961–963 (1997).

[4] J.C. Knight, T.A. Birks, R.F. Cregan, P.S.J. Russell, and J.P. de Sandro, "Large mode area photonic crystal fiber", *Elect. Lett.* 34, 1347–1348 (1998).

[5] T. M. Monro and H. Ebendorff-Heidepriem, "Progress in microstructured optical fibers" *Annu. Rev. Mater. Res.* 36, 467–495 (2006).

[6] T.A. Birks, D. Mogilevstev, J.C. Knight, and P.St.J. Russell, "Dispersion compression using single material fibers", *Photon. Technol. Lett.* 11, 674–676 (1999).

[7] A. Ferrando, E. Silvestre, J. Miret, and P. Andrés, 'Nearly zero ultraflattened dispersion in photonic crystal fibers", *Opt. Lett.* 25, 790–792 (2000).

[8] J.K. Ranka, R.S. Windeler, and A.J. Stentz, "Visible continuum generation in air silica microstructure optical fibers with anomalous dispersion at 800 nm", *Opt. Lett.* 25, 25–27 (2000).

[9] I. Hartl, X.D. Li, C. Chudoba, R.K. Ghanta, T.H. Ko, and J.G. Fujimoto, "Ultrahighresolution optical coherence tomography using continuum generation in an air-silica microstructure optical fiber", *Opt. Lett.* 26, 608–10 (2001).

[10] R.E. Drullinger, S.A. Diddams, K.R. Vogel, C.W. Oates, and E.A. Curtis, "All-optical atomic clocks", *Proc. 2001 IEEE Int. Freq. Control Symp.* 1, 69–75 (2001).

[11] T.M. Monro, S. Warren-Smith, E.P. Schartner, A. Francoiset, S. Heng, H. Ebendorff-Heidepriem, and S.V. Afshar, "Sensing with suspended-core optical fibers", *Opt. Fiber Technol.* 16, 343–356 (2010).

[12] T.R. Woliński, P. Lesiak, and A.W. Domański, "Polarimetric optical fiber sensors of a new generation for industrial applications", *Bull. Pol. Ac.: Tech.* 56, 125–132 (2008).

[13] F. Benabid, J.C. Knight, G. Antonopoulos, and P.St.J. Russell, "Stimulated Raman scattering in hydrogen-filled hollow-core photonic crystal fiber", *Science* 298, 399–402 (2002).

[14] P.S. Light, F. Benabid, F. County, M. Maric, and A.N. Luiten, "Electromagnetically induced transparency in Rb-filled coated hollow-core photonic crystal fiber", *Opt. Lett.* 32, 1323–1325 (2007).

[15] M. Bajcsy, S. Hofferberth, V. Balic, T. Peyronel, M. Hafezi, A.S. Zibrov, V. Vuletic and M. D. Lukin, "Efficient all-optical switching using slow light within a hollow fiber", *Phys. Rev. Lett.* 102, 203902 (2009).

[16] K. Kishor, R.K. Sinha, A.D. Varshney, and J. Singh, "Characterization of specially designed polarization maintaining photonic crystal fiber from far field radiation patterns", *Opt. Commun.* 283, 5007–5011 (2010).

[17] M. Szustakowski, N. Palka, and W. Grabiec, "Simple method for determination of photonic crystal fibers geometry", *Proc. of SPIE* 6588, 65880M-1 (2007).

[18] S. K. Varshney and R.K. Sinha, "Characterization of photonic crystal fibers from far field measurements", *J. Microwaves and Optoelectr.* 2, 32–42 (2002).

[19] W.A. Gambling, D.N. Payne, H. Matsumura, and R.B. Dyott, "Determination of core diameter and refractive-index difference of single-mode fibres by observation of the far-field pattern", *IEE J. Microwaves Optic Acoust.* 1, 13–17 (1976).

[20] A.K. Ghatak, R. Srivastava, I.F. Faria, K. Thyagarajan, and R. Tewari, "Accurate method for characterizing single-mode fibers – theory and experiment", *Electr. Lett.* 19, 97–98 (1983).

[21] A.C. Boucouvalas, "Use of far-field radiation-pattern to characterize single-mode symmetric slab waveguides", *Electr. Lett.* 19, 120–121 (1983).

[22] G.S. Wiederhecker, C.M.B. Cordeiro, F. County, F. Benabid, S.A. Maier, J.C. Konight, C.H.B. Cruz, and H.L. Fragnito, "Field enhancement within an optical fibre with a subwavelength air core", *Nat. Photon.* 1, 115–118 (2007).

[23] T. M. Monro, D.J. Richardson, and P.J. Bennett, *Electr. Lett.* 35, 1188–1189 (1999).

[24] T. Pustelny and M. Grabka, *Acta Phys. Pol.* A 114, A113–A118 (2008).

[25] J. Wojcik, P. Mergo, M. Makara, K. Poturaj, L. Czyzewska, J. Klimek, and A. Walewski, "Technology of suspended core microstructured optical fibers for evanesced wave and plasmon resonance optical fiber sensors", *Proc. SPIE* 6990, 6990T (2008).

[26] N.A. Mortensen and J.R. Folkenberg, "Near-field to far-field transition of photonic crystal fibers: symmetries and interference phenomena", *Opt. Express* 10, 475–481 (2002).

[27] M. Grabka, B. Wajnchold, S. Pustelny, W. Gawlik, K. Skorupski, and P. Mergo, "Experimental and theoretical study of light propagation in suspended-core optical fiber", *Acta Phys, Pol.* A 18, 1127–1132 (2010).

[28] B.E.A. Saleh and M.C. Teich, *Fundamentals of Photonics*, Wiley, New Jersey, 2007.